Investigation of LOCSET technique for precision phase control in Coherent beam combined high power fiber amplifiers

A Project Report

submitted by

DATTATREYA MAJUMDAR

in partial fulfilment of the requirements
for the award of the degree of

MASTER OF TECHNOLOGY

DEPARTMENT OF ELECTRICAL ENGINEERING
INDIAN INSTITUTE OF TECHNOLOGY MADRAS.

May 2016

THESIS CERTIFICATE

This is to certify that the thesis titled **Investigation of LOCSET technique for precision phase control in Coherent beam combined high power fiber amplifiers**, submitted by **Dattatreya Majumdar**, to the Indian Institute of Technology, Madras, for the award of the degree of **Master of Technology**, is a bona fide record of the research work done by him under my supervision. The contents of this thesis, in full or in parts, have not been submitted to any other Institute or University for the award of any degree or diploma.

Dr. Balaji Srinivasan
Project Supervisor
Associate Professor
Dept. of Electrical Engineering
IIT-Madras, 600 036

Place: Chennai

Date: 4^{th} May 2016

ACKNOWLEDGEMENTS

My sincere thanks to Dr. Balaji Srinivasan who as my project supervisor always motivated me to strive for the best. He has always supported me and instilled in me the courage in overcoming various constraints throughout my project tenure. I would also like to convey my gratitude to my lab-mates. In this regard I would like to mention Bhargav who has always been there to provide more in-depth analysis of my work and making me understand the basics of my work. Even in my hardest of times during my project he has been steadfast in guiding me and even after a long day of work he would come to my room and discuss how I could address the problem in hand. The next individual who has been closest to me is Pabitro, from whom I have acquired a more pragmatic view of my project topic. He always encouraged me to push my limits further up and made me believe that there is always a solution to a problem however hard it may seem. I am also highly grateful to Srijith, Debdatta and Guru for supporting me in my experiments from time to time. Without their help my project would not have gone so smoothly. In this context I would like to express my gratitude to Suresh Kumar S. who helped me a lot in customising the modulator cover for its proper protection. Manas and Yusuf have also been very supportive and the technical discussions with them have always been fruitful. My other friends Srinivas, Vinod, Pankaj, Raghu have stood by me to provide me with the mental support and self-belief and I also shared many light moments with them especially in the tea-corner.

I would like to sign off saying that all I am today I completely owe to my parents. Their love and support can never be quantified. Infact they have been very patient in tolerating my histrionics and mood swings from time to time and have always been my pillars of support.

ABSTRACT

KEYWORDS: Beam quality ; Coherent Beam Combining; LOCSET.

High power fiber lasers are being used in various applications owing to their excellent beam quality ($M^2 < 1.2$) and high wall-plug efficiency ($> 30\%$) while providing low cost of ownership. However, output power from a single fiber laser/amplifier is limited to kW due to limitations attributed primarily to nonlinear effects and thermal mode instability the total output power that may be extracted from a single fiber laser is only in the order of kWs, hence for applications such as directed energy in defence it is necessary to combine several fibre lasers. One promising beam combination technique is Coherent Beam Combining (CBC), in which several fiber amplifiers are phase locked with respect to each other.

A key aspect of CBC is to track the phase changes in the different fiber amplifiers and maintain phase locking. To track the phase changes photo-detectors are incorporated, but when we need to scale a large number of fiber amplifiers it becomes cumbersome to use photo-detectors for each of them. It also increases the foot-print of the system. To overcome this problem, a robust phase locking mechanism, Locking of Optical coherence via Single Detector Electronic frequency Tagging (LOCSET) is implemented where by using a single detector we can track the phase changes in each of the fibre amplifiers. Moreover, it does not require any separate reference beam to phase lock the fibre lasers.

TABLE OF CONTENTS

LIST OF TABLES

LIST OF FIGURES

ABBREVIATIONS

RF	Radio Frequency
LOCSET	Locking of Optical Coherence via Single Detector Frequency Tagging
CBC	Coherent Beam Combining
MOPA	Master Oscillator Power Amplifier
PM	Phase Modulator
EOM	Electro-Optic modulator
PD	Photo-detector
DSO	Digital Signal Oscilloscope
ESA	Electrical Spectrum Analyser
VOA	Variable Optical Attenuator
PZT	Piezo Electric Transducer
FBG	Fibre Bragg Grating

CHAPTER 1

INTRODUCTION

1.1 Motivation

In applications such as Directed Energy weapons where a large output power is necessary high power fiber lasers can play a pivotal role. This can be attributed due to the following reasons mentioned below:-(1)

- They provide a very good beam quality ($M^2 < 1.2$).M^2 is the measure of how much a beam is similar to a diffraction limited Gaussian beam ($M^2 = 1$).
- They provide a high wall plug efficiency ($> 30\%$).
- They are highly compact as compared to rod lasers or gas lasers of comparable power.
- They have a higher cooling capacity due to larger surface to volume ratio of fiber geometry as compared to other lasers.

But inspite of these advantages fibre lasers have their own limitations. A single fiber laser cannot be scaled to higher levels of power (even to kWs of power).The two primary reasons being:-

- Non linear effects mainly Stimulated Brillouin Scattering play a detrimental role in case of narrow line width lasers and hence affecting the source itself.
- Thermal mode instability is the other constraint. When we try to operate the fiber laser at higher power levels the fiber core is no longer single mode instead it becomes multi-mode i.e. together with LP_{01} fundamental mode we also have higher order modes such as LP_{11} which eventually degrades the beam quality.

So to mitigate this problem we need to implement beam combining of several lasers to scale to higher levels of power. Beam combining can be implemented by various methods such as spatial combining, spectral combining and coherent combining. In case of spatial combining the constraint lies in the alignment of the free space optics as we are trying to combine several laser sources spatially to a single point. Moreover the effective length of these amplifiers vary which lead to a relative phase change which eventualy degrades the beam quality and also the net output power. Coming to spectral

beam combining this involves combining several laser emitters of specific wavelengths into a single beam. In order to achieve high-density combining of many individual lasers, a combining element with high resolving power, such as a diffraction grating, is required. But this technique cannot be utilised in scaling large number of fibre lasers. So a suitable method is required with which we can scale several of fibre lasers and at the same time phase lock each of the fiber amplifiers. This is where coherent beam combining comes into play where all elements of the laser array are forced to operate with the same frequency spectrum and with the same phase, so that when the beams are overlapped, the optical fields add to provide constructive interference.(1),(4)

1.2 Background

To implement CBC an important component to track the phase change is the photodetector, yielding a photocurrent, with the help of which the phase error signal corresponding to a single element of the fibre laser array is fed back. CBC can be implemented by several approaches as discussed below briefly:-(1)

- Common resonator - Array elements are placed inside an optical resonator and feedback from the resonator is used to couple the elements together.
- Evanescent or leaky-wave coupling - In this approach the array elements are placed sufficiently close together so that their field distributions overlap, thereby coupling the elements. In-phase coupling of the array elements is desired to obtain high on-axis far-field intensity.
- Self- organization - This involves array comprising elements with very different optical path lengths, and the optical spectrum self-adjusts to minimize the loss of the array
- Active feedback - In this method the laser elements are individually phase controlled and feedback is used to equalize the optical path lengths.

Active control of phase is primarily used mainly because in case of passive phase control scalability to large optical arrays is not possible. In active CBC implementation the individual optical array elements or laser elements are phase controlled and feedback is used to equalize the optical path lengths modulo 2π. In case of large fibre laser arrays, comprising several fibre lasers, it becomes cumbersome to incorporate photodetectors for each of the lasers. Herein the technique *Locking of Optical coherence via Single Detector Electronic frequency Tagging* (LOCSET) is unique where by using only

a single photo-detector we can track the relative phase in each of the arms of the fiber amplifier array.

1.3 Phase error variation with number of optical elements in CBC

In case of coherent beam combining one of the most vital parameters that determines its performance is the beam combining efficiency which is defined as the fraction of the output power to the total input power. But if we consider all the input powers to be equal then the beam combining efficiency is then governed by the sustainable RMS phase error in the co-related case i.e. the phase locked condition. A simple expression for the beam combining efficiency is given in Eqn. 1.1 (2),(3).

$$\eta = \frac{1}{N} \frac{|\sum_{m=1}^{N} \sqrt{P_m} exp(j\Delta\phi_m)|^2}{\sum_{m=1}^{N} P_m} \tag{1.1}$$

But here we will like to express the beam combining efficiency in terms of the Strehl‘s ratio because in case of tiled apertures the beam combining efficiency is equivalent to the Strehl‘s ratio. Strehl‘s ratio can be defined as the ratio of the peak far-field intensity of a beam divided by the peak intensity from a uniformly illuminated aperture having the same total power. The Strehl‘s ratio depends on the number of optical array elements and the RMS phase error. The Strehl‘s ratio (S) for the one-dimensional correlated case is expressed in Eqn. 1.2.

$$S = \frac{-2\alpha + 2\alpha^{N+1} + N - N\alpha^2}{N^2(1-\alpha)^2} \tag{1.2}$$

In Eqn. 1.2, N is the number of array elements and $\alpha = exp(\frac{-\sigma_\phi^2}{2})$ where σ_ϕ is the standard deviation of ϕ. So from Eqn. 1.2 by predefining a certain S and N we can obtain σ_ϕ. However when we consider higher number of optical elements Eqn. 1.2 gets modified to Eqn. 1.3.

$$S = \frac{4}{N\sigma_\phi^2} \tag{1.3}$$

The plot in Fig. 1.1 shows the variation of σ_ϕ with N for $S = 0.9$.

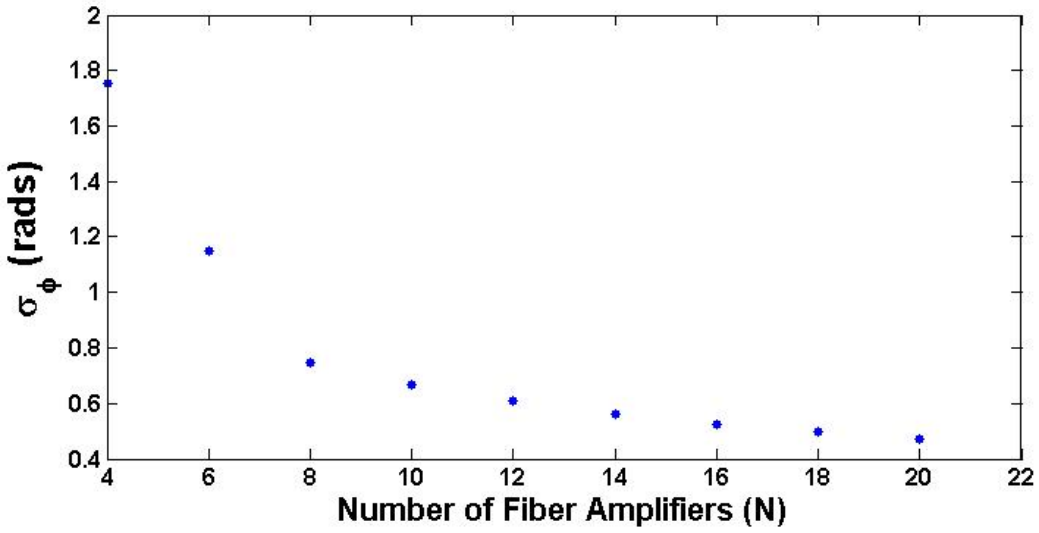

Figure 1.1: Varaition of σ_ϕ with N for S=0.9

From the plot it is clearly evident that after N=7 the variation pattern of σ_ϕ with N changes and eventually it saturates for higher values of N. So to get rid of these phase errors which eventually degrade the output power and the beam quality we need to implement CBC using a much robust phase locking mechanism. This is where LOCSET comes into play.

1.4 LOCSET Theory

In our project we have implemented CBC by using the LOCSET technique. This novel coherent beam combining system offers a highly accurate and robust phase locking mechanism. Moreover the technique also provides a scalability of over 100 elements(4). Another advantage of this technique over other phase array locking systems is that it does not require an external reference beam.

In this technique a master oscillator power amplifier (MOPA) configuration is employed where a narrow line-width laser seeds an array of fiber amplifiers. After that every beam of the optical array is phase modulated at a unique radio frequency (RF). Then a certain portion of each beam is then sampled and directed onto a single far-field photo-detector. This interference signal is then processed by feedback electronics where the relative phase error of each element with respect to all other elements are electronically isolated or demodulated. The basic schematic diagram of the LOCSET

technique is depicted in Fig 1.2:-(4)

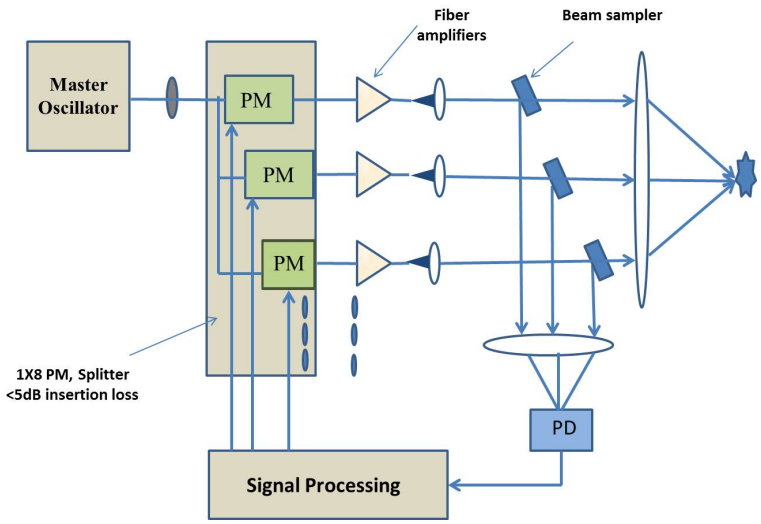

Figure 1.2: Schematic of LOCSET technique

LOCSET has two configurations a) self-referenced and b) self-synchronous. The basic difference between the two techniques is that in the case of the self-referenced model an un-modulated beam is used as a reference beam while in the case of the self-synchronous model all the beams are phase modulated. In the self referenced case the difference between the phase modulated elements and the un-modulated element is estimated and henceforth the phase locking is implemented such the relative phase error is zero. On the other hand in the self-synchronous mechanism all the beams are phase modulated. To carry out phase locking for this case we obtain the mean phase of all the optical array elements and thereby try to phase lock the phase spectrum relative to the mean(4). To understand this more clearly we can use a phase plot to understand the phase locking methodology more clearly.

The schematic shown in Fig 1.3 will illustrate the difference between the two methods:-

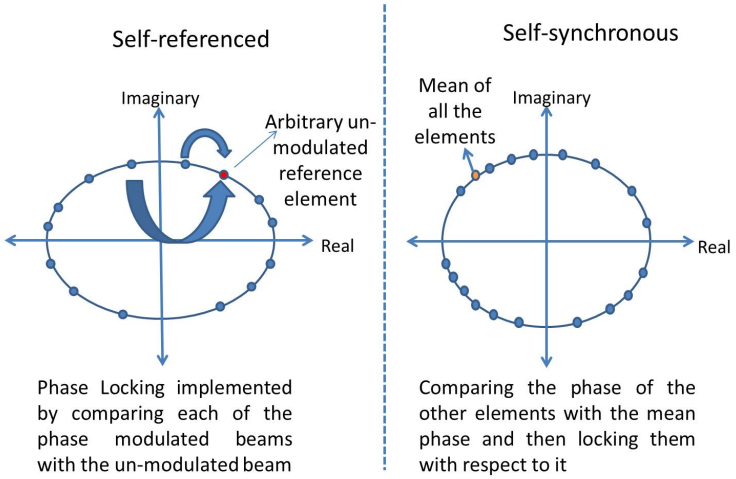

Figure 1.3: Phase locking schematics of LOCSET

In Fig 1.3 the two phase plots illustrate the phase locking schemes for the two methods. As discussed earlier we can see that for the self-referenced case all the other array elements are phase locked to the initial phase of the un-modulated array element. On the other hand for the self-synchronous case we are first evaluating the mean phase of all the array elements and thereby locking the phase of the array elements to it.

1.5 Objectives

- Implement the LOCSET algorithm in a MATLAB-SIMULINK model and understand the phase locking requirements.
- Demonstrate the LOCSET algorithm through controlled experiments

1.6 Organisation of Report

Our project involved simulations and experiments based on the self-referenced and self-synchronous LOCSET models. As a part of our simulations we implememted the 2-beam Self-referenced LOCSET model on MATLAB-SIMULINK and giving various input phase arrays we have tried to estimate the phase at output which we will be discussing in the next chapter. Our experiments mainly focus on establishing the 2-beam self referenced and 2-beam self-synchronous cases and to once again estimate

the phase at the output by using their individual RF spectrums on the Electrical Spectrum Analyser (ESA). We also provided additional phase in one of the arms of the self-synchronous case and measured the change in the estimated phase.Finally we will summarise our results and also discuss about the future course of this work.

CHAPTER 2

Simulations of LOCSET Algorithm

Before going into the simulation models which we designed in MATLAB-SIMULINK, we will try to understand the basic theory governing the LOCSET operation. As we are combining several fibre lasers it is important to know the optical field coming out of each of them. These optical beams are made incident on a photo-detector which generates a photocurrent. Therefore we need to formulate the resultant photocurrent eventually from which we would be able to estimate the phase at the output.

2.1 Optical Field

For the self-referenced technique there are N-1 phase modulated beams and one un-modulated beam given by E_i(t) and E_u(t) respectively. The fields are defined below:-

$$E_u(t) = E_{u0}cos(\omega_L t + \phi_u(t)) \tag{2.1}$$

$$E_i(t) = E_{i0}cos(\omega_L t + \phi_i(t) + \beta_i sin(\omega_i t)) \tag{2.2}$$

Here E_{u0} and E_{i0} are the field amplitudes of the un-modulated and phase modulated beams, ω_L is proportional to the shared frequency of the optical beams and $\phi_u(t)$ and $\phi_i(t)$ are slowly varying phase states of the un-modulated and phase modulated beams respectively. $\beta_i sin(\omega_i t)$ represents an applied sinusoidal phase modulation with amplitude β_i and unique RF frequency ω_i.It is this unique RF frequency phase modulation that allows us to later demodulate the phase error of the ith beam with respect to all other beams in the array. It can be assumed that $\phi_u(t)$ and $\phi_i(t)$ are constants as they vary much slowly than the optical frequency, and RF phase modulation frequencies are defined momentarily. For simplicity we must assume that all the beams have common optical properties and propagate along a common spatial path to the photo-detector.

Thus we can write finally a combined electric field expression:-(4),(5)

$$E_T(t) = E_u(t) + \sum_{i=1}^{N-1} E_i(t) \tag{2.3}$$

2.2 Photocurrent

The basic photo-current equation is given by the expression below where A is the active area of the photo-detector, R_{PD} is the responsivity of the photo-detector and I(t) is the time varying intensity of the combined beams:-(4),(5)

$$i_{PD}(t) = R_{PD}AI(t) \tag{2.4}$$

where I(t) is given by:-

$$I(t) = \frac{1}{2}(\frac{\epsilon_0}{\mu_0})^{\frac{1}{2}}(E_T^2) \tag{2.5}$$

Eventually after expanding (1.4) after putting I(t) in it we obtain:-

$$i_{PD}(t) = R_{PD}A\frac{1}{2}(\frac{\epsilon_0}{\mu_0})^{\frac{1}{2}}[E_u^2(t) + 2E_u(t)\sum_{i=1}^{N-1} E_i(t) + (\sum_{i=1}^{N-1} E_i(t))(\sum_{j=1}^{N-1} E_j(t))] \tag{2.6}$$

The first summation on the right multiplied with the un-modulated electric field gives the photo-current due to the un-modulated reference beam interfering with each of the phase modulated beams and can be denoted as $i_{uj}(t)$.

$$i_{uj}(t) = R_{PD}A\frac{1}{2}(\frac{\epsilon_0}{\mu_0})^{\frac{1}{2}}2E_u(t)\sum_{i=1}^{N-1} E_i(t) \tag{2.7}$$

Ignoring the photocurrent terms oscillating at the frequency of the laser and applying trigonometric identities and expressing the following trigonometric quantities as a Fourier series expansion of their Bessel terms we obtain:-

$$cos(\beta_i sin(\omega_i t)) = J_0(\beta_i) + 2\sum_{n=1}^{\infty} J_{2n}(\beta_i)cos(2n\omega_i t) \tag{2.8}$$

$$sin(\beta_i sin(\omega_i t)) = 2\sum_{n=1}^{\infty} J_{2n-1}(\beta_i)sin((2n-1)\omega_i t) \tag{2.9}$$

Thus the final expression of the photocurrent due to the beating of the un-modulated beam with phase modulated beams is:-(4),(5)

$$i_{uj}(t) = R_{PD}(P_u)^{\frac{1}{2}} \sum_{i=1}^{N-1} (P_i)^{\frac{1}{2}} (cos(\phi_u - \phi_i)(J_0(\beta_i) + 2\sum_{n=1}^{\infty} J_{2n}(\beta_i) cos(2n\omega_i t)) + sin(\phi_u - \phi_i)(2\sum_{n=1}^{\infty} J_{2n-1}(\beta_i) sin((2n-1)\omega_i t)))$$

where

$$P_u = \frac{A(E_{u0})^2}{2} (\frac{\epsilon_0}{\mu_0})^{\frac{1}{2}} \tag{2.10}$$

2.3 Phase error control signal

Our next aim is to extract the phase control signal which will eventually lead us to the phase error measurement. This is done by coherent demodulation in the RF domain. In this method we can find the phase control signal for a particular ith element of the array by multiplying the photocurrent by $\sin(\omega_i t)$ and integrated over a time τ, where ω_i represents the frequency of one of the phase modulated elements. The integration time,τ , is selected long enough to isolate the individual phase control signals of the phase modulated elements and short enough so that the phase control loop can effectively cancel the phase disturbances of the system (4),(5). The phase control signal of the ith element of the self-referenced LOCSET systems is given by:-

$$S_{Si} = \frac{1}{\tau} \int_0^{\tau} i_{PD}(t) \sin(\omega_i t) dt \tag{2.11}$$

where S_{Si} is the phase error control signal. For the self-referenced case the phase error control signal S_{SRi} is given as :-

$$S_{SRi} = R_{PD} \sqrt{P_i} J_1(\beta_i) [\sqrt{P_u} \sin(\phi_u - \phi_i) + \sum_{j=1}^{N} \sqrt{P_j} J_0(\beta_j) \sin(\phi_j - \phi_i)] \tag{2.12}$$

By using the error signal in Eqn 2.12 in the feedback control loop the phase is locked. In this mode the phases of the phase modulated array elements are adjusted by the feedback loop to track the phase of the unmodulated element. Therefore, the relative phases between the unmodulated array element and each of the phase modulated array ele-

ments at the sensing photodetector are preserved when any or all of the array elements are disturbed.

2.4 MATLAB-SIMULINK model

As a part of our simulation we replicated the 2-beam self referenced LOCSET model on MATLAB-SIMULINK. The model implemented on SIMULINK gives two optical fields as input i.e. the optical fields corresponding to the un-modulated and phase modulated beams.Eventualy we carry out the square of the modulus of the resultant optical field and multiplying with responsivity we finally obtain the photo-current response in the time domain. The SIMULINK model illustrating the same is shown in Fig 2.1:-

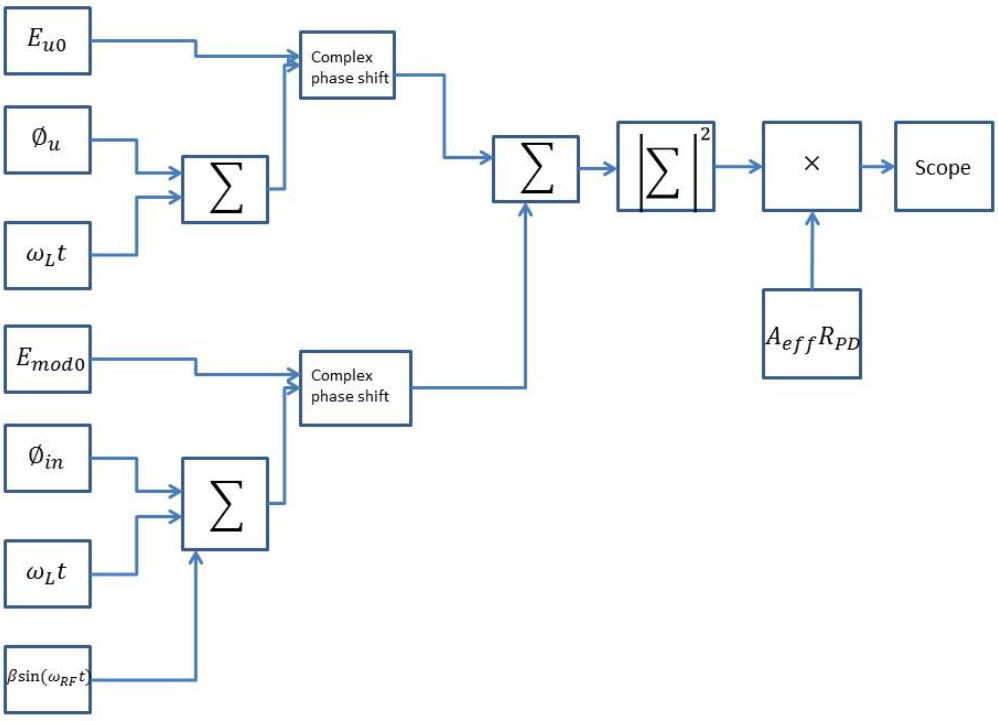

Figure 2.1: SIMULINK model for 2-beam self-referenced LOCSET

In Fig 2.1 the term ϕ_u is a constant which is the initial phase of the un-modulated beam. In our simulations we have taken ϕ_u to be 0. The variable ϕ_{in} is the discrete phase being applied to the modulated beam and this term we will keep on varying taking into consideration different input phase arrays. The block labeled the phase modulation term represents the $\beta sin(\omega_{RF}t)$. Here we have kept $\beta = 0.1$ and $\omega_{RF} = 2MHz$. Finally the

scope gives us the photo-current response in the time domain which eventually helps us in the phase estimation.

2.5 Phase Estimation from the photocurrent

From the expression of the photocurrent it is evident that the odd order Bessel terms are the coefficients for the sine of the relative phase of the un-modulated and modulated element and similarly the even order Bessel terms are the coefficients for the cosine of the relative phase. So our aim is to estimate the phase from the photocurrent and check whether it matches with the given input phase. The phase extraction process involves performing a Fast Fourier Transform of the photocurrent and then extract the Bessel components $J_1(\beta)$ and $J_2(\beta)$ from the FFT spectrum which are the peaks corresponding to ω_{RF} and $2\omega_{RF}$ respectively. Our next step involves calculating the ratio $\frac{J_1(\beta)}{J_2(\beta)}$ and then plot it with respect to the individual phase values. The nature of the curve will be similar to that of a tan curve. Now by fitting this curve to a tan equation and inserting $\frac{J_1(\beta)}{J_2(\beta)}$ back into the equation we try to estimate the phase at the output. The schematic of phase estimation is explained in Fig 2.2:-

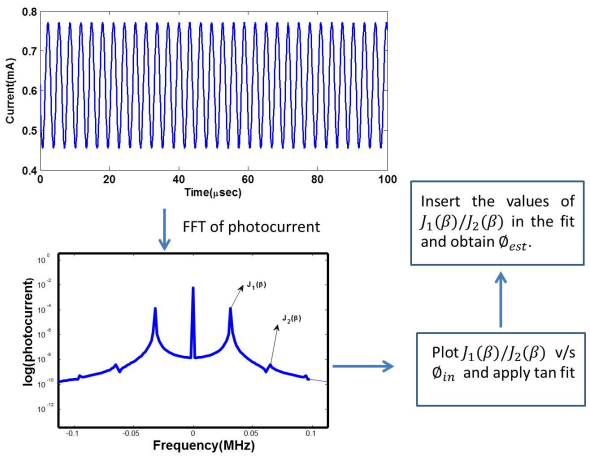

Figure 2.2: Phase Extraction Schematic

In this regard we carried out two analyses to demonstrate the phase estimation.

2.5.1 Phase analysis 1

Here we took an input phase array from 0 to π in steps of $\frac{\pi}{100}$ and fed it into the block of ϕ_{in} and tried to estimate the phase at the output. We plotted the variation of the phase error with respect to input phase.

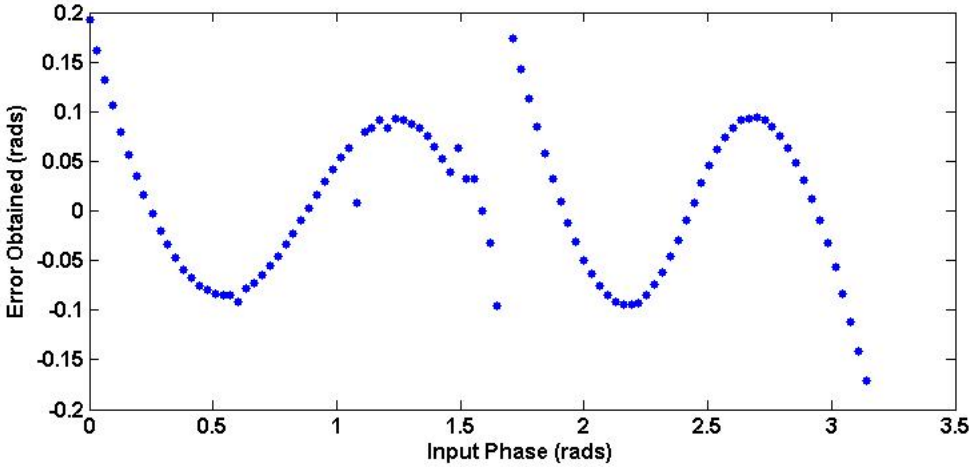

Figure 2.3: Variation of phase error with input phase

In Fig 2.3 it is evident that we are obtaining a symmetric distribution of the phase error from 0 to π/2 and after π/2 to π. But it is also evident from Fig 2.3 for certain input phase values such as 0, π/2 and π the phase error is too high. So estimate the phase at these values we need to consider single Bessel component. Hence the resultant photo-current equation in these cases will also change. The single Bessel component estimation for the above mentioned three values is discussed below:-

- For $\phi_{in} = 0$, $J_2(\beta)$ is much larger compared to $J_1(\beta)$. So here we will consider only $J_1(\beta) = 8.14 \times 10^{-8}$. Thus the photocurrent equation turns out to be:-

$$i_{PD}(t) = 2R_{PD}P_u(8.14 \times 10^{-8}) \sin(\phi_{est}) \sin(\omega_{RF}t) \tag{2.13}$$

- For $\phi_{in} = \pi/2$, $J_1(\beta)$ is much larger compared to $J_2(\beta)$. Hence the Bessel component taken into account in this case is $J_2(\beta) = 1.41 \times 10^{-4}$. Eventually the photocurrent equation turns out to be:-

$$i_{PD}(t) = 2R_{PD}P_u(1.41 \times 10^{-4}) \cos(\phi_{est}) \cos(2\omega_{RF}t) \tag{2.14}$$

- Finally for the last case i.e. for $\phi_{in} = \pi$, $J_2(\beta)$ is much larger compared to $J_1(\beta)$. Therefore the Bessel component considered here also is $J_1(\beta) = 8.14 \times 10^{-8}$. So the photocurrent obtained in this case is:-

$$i_{PD}(t) = 2R_{PD}P_u(8.14 \times 10^{-8}) \sin(\phi_{est}) \sin(\omega_{RF}t) \tag{2.15}$$

So thereby taking into account the single Bessel component analysis for those input phase values where the phase error is too high, we obtained a modified phase error vs input phase applied plot.

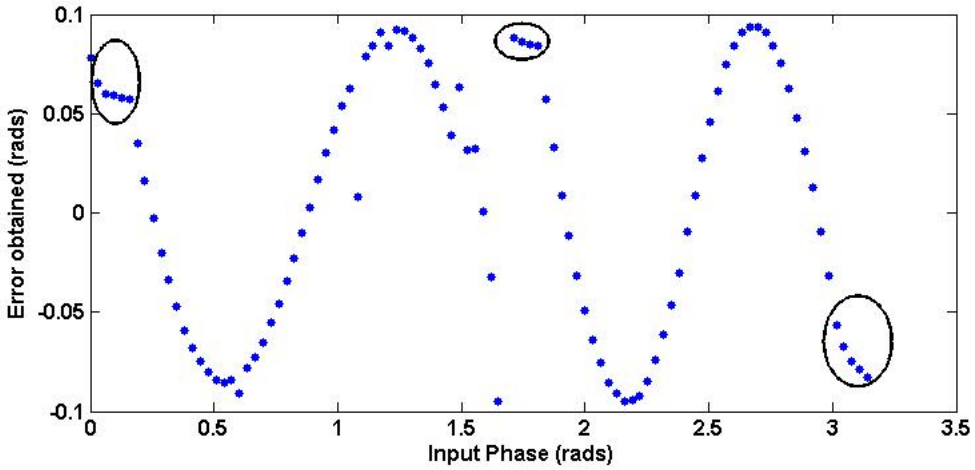

Figure 2.4: Variation of phase error with input phase after applying single Bessel component analysis

From Fig 2.4 we can see the points encircled are those corresponding to the single Bessel component analysis.The phase error evaluated now is much more negligible than that in Fig 2.3 and hence the analysis is validated.

2.5.2 Phase analysis 2

In this analysis we have generated random Gaussian phase arrays and given them as input to the phase of the modulated element. Hence we took 4 such random Gaussian phase arrays with different mean input phase values i.e. different $\overline{\phi_{in}}$ corresponding to the SIMULINK model. Thereafter following the same phase extraction schematic we found out the mean estimated phase, $\overline{\phi_{est}}$, from the photocurrent equation. So in this analysis we will focus on the deviation of the mean of the estimated phase, the number of phase samples retrieved back and whether the Gaussian distribution is also maintained for the estimated phase array.

The four different cases are discussed below:-

- $\overline{\phi_{in}} = 0.8$ $\overline{\phi_{est}} = 1.06$

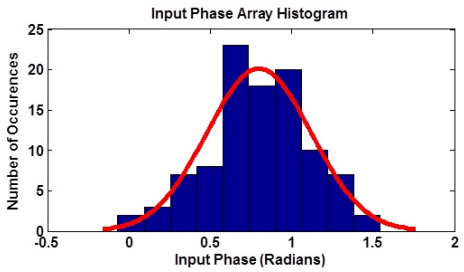

Figure 2.5: Input phase array histogram for $\overline{\phi_{in}} = 0.8$

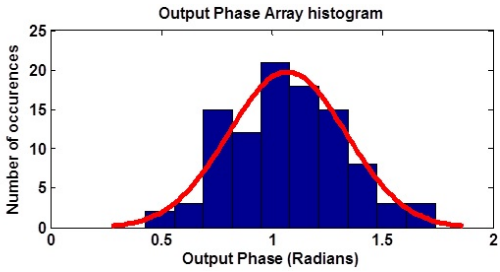

Figure 2.6: Estimated phase array histogram $\overline{\phi_{est}} = 1.06$

Analysis - For the first case we can see that estimated phase at the output is also Gaussian in nature. All the phase samples were estimated back at the output. But the error or deviation in this case was too high (approximately 0.2 rads)

- $\overline{\phi_{in}} = 1.57$ $\overline{\phi_{est}} = 1.484$

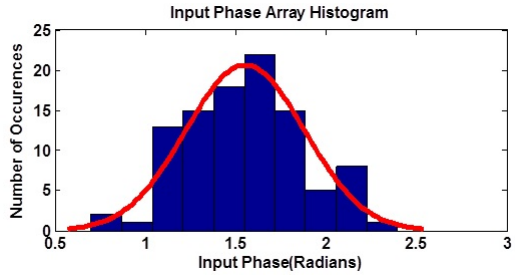

Figure 2.7: Input phase array histogram for $\overline{\phi_{in}} = 1.57$

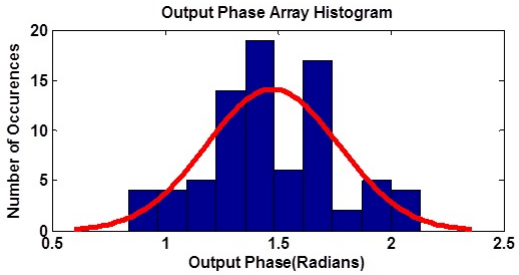

Figure 2.8: Estimated phase array histogram for $\overline{\phi_{est}} = 1.484$

Analysis - In this case we see that we are unable to extract a majority of the input phase values which are in the vicinity of $\pi/2$ as the Bessel ratios are blowing up. Physically this suggests that for a phase value in the proximity of $\pi/2$ is resulting in destructive interference and thus we are unable to extract the phase which we are giving as input.

- $\overline{\phi_{in}} = 1.8$ $\overline{\phi_{est}} = 1.83$

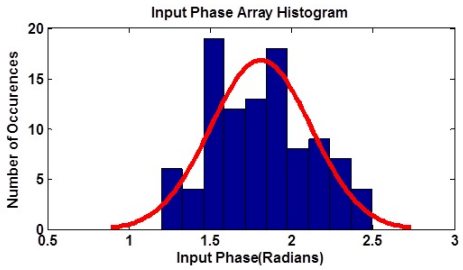

Figure 2.9: Input phase array histogram for $\overline{\phi_{in}} = 1.8$

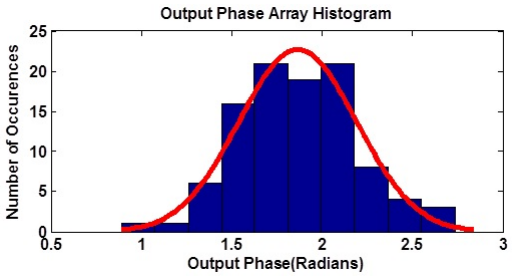

Figure 2.10: Estimated phase array histogram for $\overline{\phi_{est}} = 1.83$

Analysis - For this case we found that the deviation of $\overline{\phi_{est}}$ from $\overline{\phi_{in}}$ was the least and we could extract all the corresponding estimated phase values for the given input phase values.

- $\overline{\phi_{in}} = 2.5$ $\overline{\phi_{est}} = 2.533$

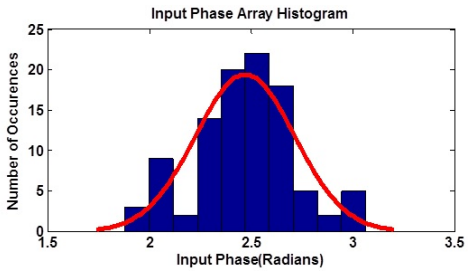

Figure 2.11: Input phase array histogram for $\overline{\phi_{in}} = 2.5$

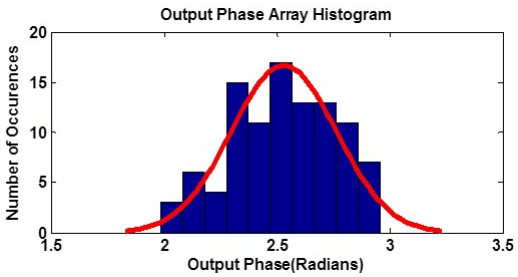

Figure 2.12: Estimated phase array histogram for $\overline{\phi_{est}} = 2.533$

Analysis - The last case that we analysed yielded us back all the corresponding output phase samples and like the previous case the deviation here also was very negligible. The distribution obtained was also Gaussian in nature.

2.5.3 Summary

We can see that LOCSET is a robust CBC technique which completely eliminates the need for a separate reference beam. The self-referenced LOCSET and self-synchronous LOCSET techniques are less complex electronic phase locking techniques than previous electronic phase locking systems. Bot these techniques have reduced the footprint of the entire system by incorporating on a single photodetector rather than N detectors for an N element array.

The basic operating principle and the theory behind LOCSET has been discussed. As a part of our simulations we have modeled the 2-beam self-referenced LOCSET on

MATLAB-SIMULINK and tried to estimate the phase at the output.The phase extraction technique employed as a part of our simulations yielded expected results and hence this Bessel component analysis was successful in estimating the phase at the output.However we found in both the analyses that in the vicinity of π/2 we were not able to estimate the phase at the output. This can be elucidated mathematically by the fact that at π/2 the Bessel components are blowing up and hence we are not being able to estimate the phase. Physically this can be interpreted as that near this phase value destructive interference might be taking place and as a result of which no photo-current is generated due to which we are unable to extract back the phase. However for most of the Gaussian phase array distributions that we gave as input we were able to get back the output Gaussian phase array distributions with slight deviations of $\overline{\phi_{est}}$ from $\overline{\phi_{in}}$. We have also characterised those input phase values for which the phase error are distinctively high and tried to estimate them from their single Bessel components. This estimation helped us to formulate the corresponding photo-current equations also for these phase values. In the following chapter we will discuss about the controlled experiments which we carried out to estimate the phase once again at the output.

CHAPTER 3

Experiments implementing LOCSET algorithm

3.1 Problem statement and constraints

In our experiments we validated the results we obtained from the simulations by implementing the basic model of 2-beam self-referenced and self-synchronous LOCSET. In the self-referenced case one of the beams will be phase modulated and the other un-modulated, whereas for the self-synchronous both of them will be phase modulated. We used Distributed Feed-back(DFB) Laser as our source. But as we did not have phase modulators, we used amplitude modulators by biasing them at the null positions to implement phase modulation.So in this regard we needed to characterise the electro-optic modulators(EOMs) and obtaining their individual V_π or null-point , i.e. voltage at which the optical power obtained from the modulator is minimum. Also we need to remove the residual amplitude modulation to achieve proper phase modulation.

So this chapter will focus on implementing the following:-

- Characterisation of EOM and indicating the bias points
- Optimization of peak-peak voltage of the RF-signal
- Observing RF spectrum for 2-beam self-referenced case
- Observing RF spectrum for 2-beam self-synchronous case and estimating the phases of the individual beams from the spectrum
- Estimation of the output phase in both arms after adding additional phase in one of the arms by applying calibrated strain using a Piezo-electric Transducer(PZT) with a fibre Bragg grating (FBG) pasted on it

3.2 Characterisation of EOM

The set-up shown in Fig 3.1 is employed to characterise the power response with respect to applied DC voltage for EOMs. The polarisation controller(PC) is used because the EOM consists of $LiNbO_3$ crystal which gives the maximum power at a certain polarisation when no bias voltage is applied to the EOM. So the PC helps in maintaining the required polarisation.The modulator that we used was of LUCENT Technologies and it was a dual drive modulator.

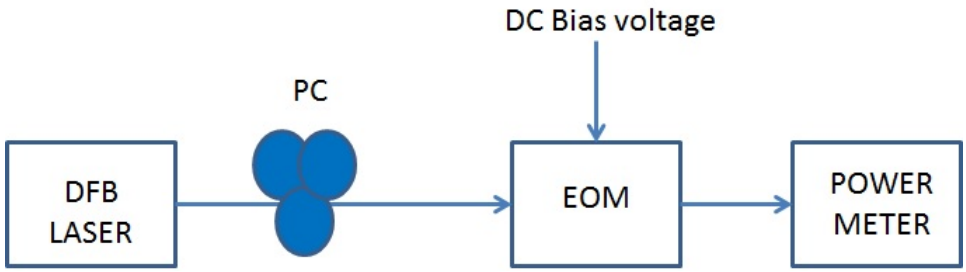

Figure 3.1: Experimental set-up for characterisation of Electro-Optic Modulator

We varied the DC bias from -4.8 V to 4.8 V in steps of 0.2 V and measured the power for each case. Eventually the variation of power with respect to the DC bias voltage was plotted as shown in Fig 3.2.

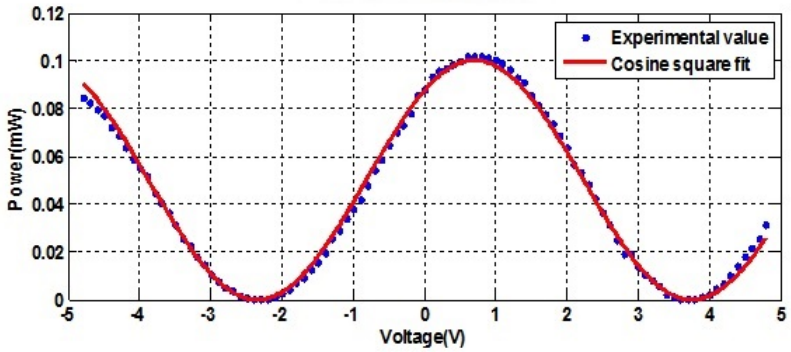

Figure 3.2: Characterisation of Electro-Optic Modulator

The variation obtained was in coherence with the theory which states that the optical power coming out of the EOM varies as the square of the cosine of the input voltage. The V_π measured from the plot was 3.1 V and the difference of the maximum and minimum power known as extension ratio was approximately 35 dB. Hence to phase modulate the EOM we need to bias it at the null point. However we should keep in mind that the null point keeps changing with respect to changes in temperature in the environment. So it is mandatory to check whether our EOM is biased at the null point

at certain time intervals. But just biasing at the null we will not be able to implement proper phase modulation because if we apply higher amplitudes in the RF signal then it is quite probable that EOM will shift from the null point and start operating in the linear region of the curve shown above. Hence we need to find out the optimum modulation amplitude of the RF signal for which the output peak-peak voltage is minimum.

3.3 Optimization of peak-peak voltage of the RF signal

As discussed earlier we need to get rid of the residual amplitude modulation. For that we need to characterise the peak-peak voltage of the RF signal and identify that maximum value for which the peak-peak voltage at the output is minimum. The set-up shown in Fig 3.3 was used to carry out the characterisation.

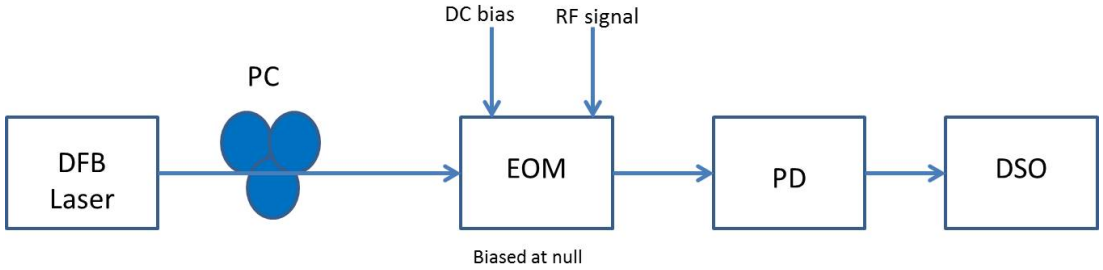

Figure 3.3: Experimental set-up for identifying the optimum RF peak-peak voltage

To estimate the optimum peak-peak modulation voltage we varied the amplitude of the RF signal from 20mV to 0.42V and measured the peak-peak voltage on the digital oscilloscope. The plot in Fig 3.4 shows the variation of the output peak-peak voltage as a function of peak-peak voltage of the RF signal.

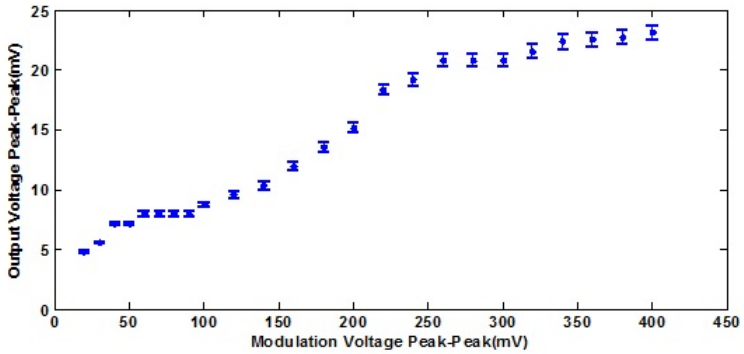

Figure 3.4: Variation of output peak-peak voltage as a function of peak-peak voltage of the RF signal

From the plot it is evident that upto 90 mV the peak-peak voltage is comparatively much small and also almost constant. Thus we choose 90 mV as the optimum peak-peak voltage of the RF signal.

3.4 2-beam Self-referenced model

To illustrate the self-referenced case, we carried out the experimental set-up shown in Fig 3.5.

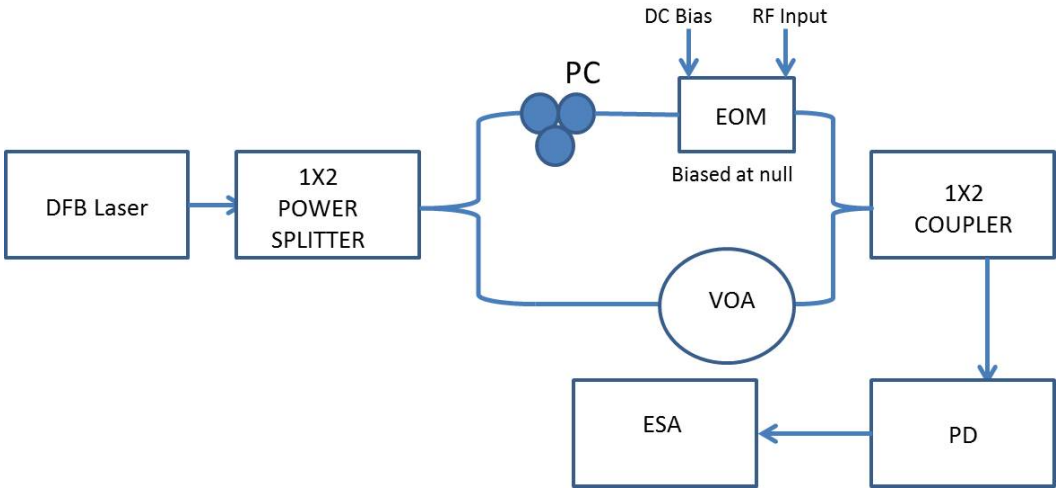

Figure 3.5: 2-Beam self-referenced model

The EOM is biased at the null-point and the RF signal has an amplitude of 90 mV at 2 MHz. The un-modulated arm plays a vital role in preserving the phase information at the output in the intensity expression in the form of $\cos^2(\frac{\phi}{2})$. The variable optical attenuator (VOA) plays a vital role here. If the second arm has too high DC power value then it will suppress the modulation component at the specific RF due to destructive interference. So we need to maintain the same optical power in both the arms to get the proper RF spectrum on the Electrical Spectrum Analyser(ESA). Thus VOA provides the necessary attenuation to the second arm and we obtain a proper RF spectrum. We carried out this experiment for two different modulation frequencies 2 MHz and 2.1 MHz.

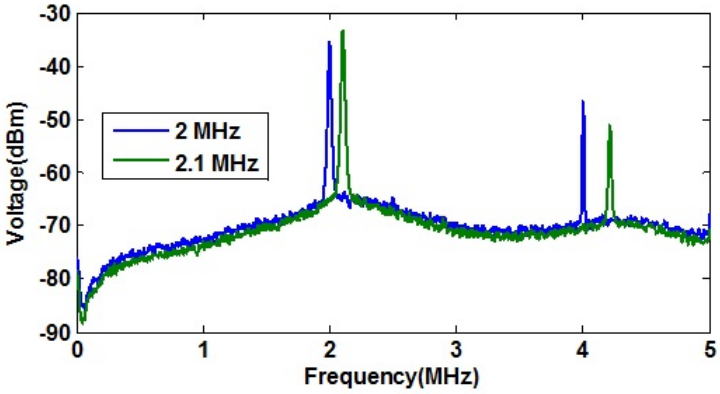

Figure 3.6: RF spectrum of 2-Beam self-referenced model for 2 and 2.1 MHz

The RF spectrum in Fig 3.6 shows peaks at both the fundamental and second harmonic for both the modulation frequencies. This is because the photo-detector is a square law detector and hence we will also obtain a peak at the corresponding second harmonic.

3.5 2-beam Self-synchronous model

The self-synchronous involves both the beams to be modulated at two different RFs. In Fig 3.7 the experimental set-up implementing 2-beam self-synchronous case is shown.

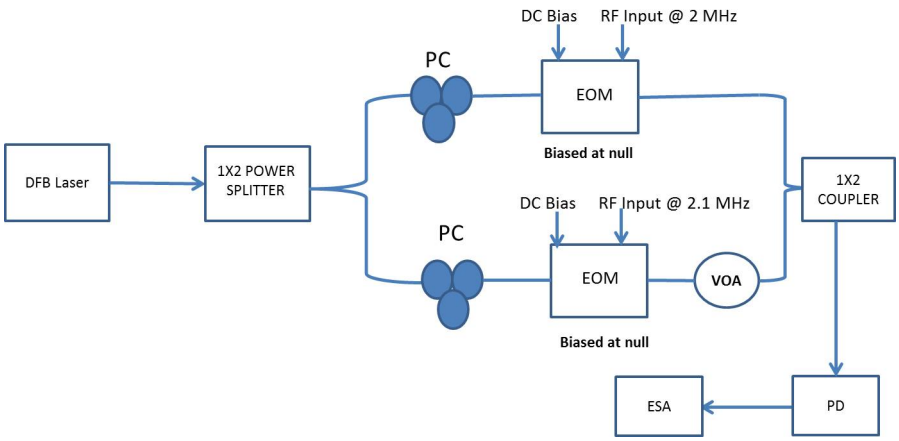

Figure 3.7: 2-Beam self-synchronous model

The two modulation frequencies should be chosen such that the fundamental of one does not overlap with higher order harmonics of the other. In our case we chose 2 MHz and 2.1 MHz respectively. The RF spectrum obtained is shown in Fig 3.8. The spectrum

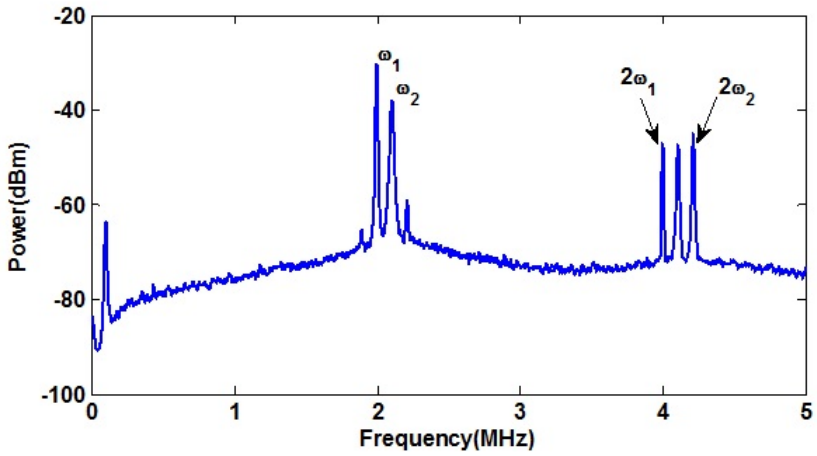

Figure 3.8: RF spectrum for 2-Beam self-synchronous model

clearly shows peaks at the fundamental and second harmonic for 2 MHz and 2.1 MHz. Along with these peaks, there are also peaks at the beat frequencies i.e. at $(\omega_1 + \omega_2)$ and $|\omega_1 - \omega_2|$ which correspond to 4.1 MHz and 0.1 MHz respectively in this case.

Our aim is to finally estimate the phase accumulated in both the beams from the RF spectrum. Analogous to the phase extraction schematic in the simulations, in experiment also we will consider the peaks corresponding to the fundamental and second harmonics, ignoring thereby the beat terms.

3.6 Phase estimation from RF spectrum

The experiments that we have carried out so far, in all these cases the modulators have been biased at the null point and hence phase modulation has been carried out. As the modulator that we are using is a dual drive modulator, biasing it at null will correspond to a phase shift of $\frac{\pi}{2}$. So $\frac{\pi}{2}$ can be termed as the input phase provided in both the arms of the 2-beam self-synchronous model shown in Fig 3.7.Our aim is to estimate the phase of both of these beams from the RF spectrum. Similar to our simulations we will estimate the peaks of the fundamental and second harmonic of the modulation frequencies from

Fig 3.8. Hence the phase accumulated in one of the beams can be estimated as

$$\tan \phi_{est} = \frac{Peak_{\omega_{RF}}}{Peak_{2\omega_{RF}}}. \tag{3.1}$$

Obtaining the peak values corresponding to $\omega_1 = 2MHz$ and $\omega_2 = 2.1MHz$ we found out that $\phi_{1est} = 1.55$ radians and $\phi_{2est} = 1.36$ radians. The phase considered as input in both the arms was approximately 1.57 radians. So the phase error incurred in the two arms are 0.02 radians and 0.19 radians. These error values are in coherence with those we had estimated from our simulations i.e. the maximum error is approximately 0.2 radians in both the cases.

3.7 Phase Estimation after adding extra phase in one of the arms

The previous section we discussed about estimating the phase at the output of both the arms. To further study this phase estimation, we incorporated the method of introducing additional phase in one of the arms and similarly evaluating its phase at the output. In order to implement this we need to add delay in that particular arm which will eventually lead to a phase change. So we used a PZT with a FBG of Bragg wavelength of 1574nm pasted on it, to provide that additional delay. The PZT expands when a certain voltage is applied to it i.e. the electric potential produces a mechanical strain which makes the PZT actuator to expand. The Thor Labs PZT that we used had a PZT coefficient of 0.116μm/V.But we needed to find out the shift of the Bragg wavelength of the FBG to determine the actual delay. For that we implemented the set-up for characterisation of FBG coefficient as shown in Fig. 3.9.

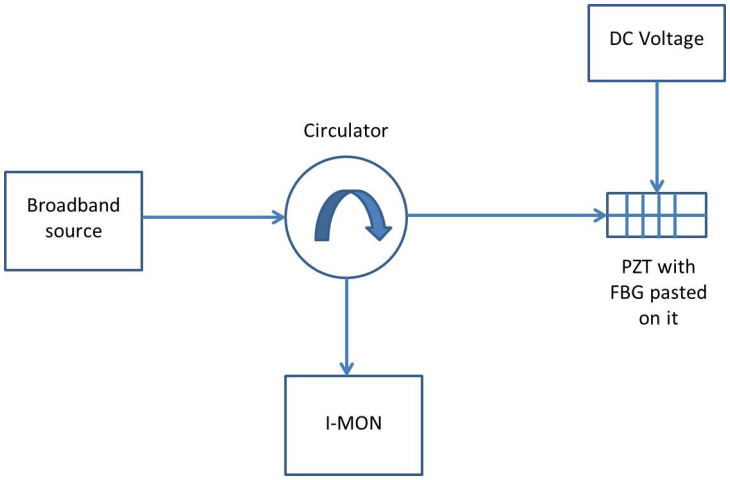

Figure 3.9: Set-up for characterisation of FBG coefficient

So by varying voltages from 0 to 30 V in steps of 5 V we obtained the plot as in Fig. 3.10

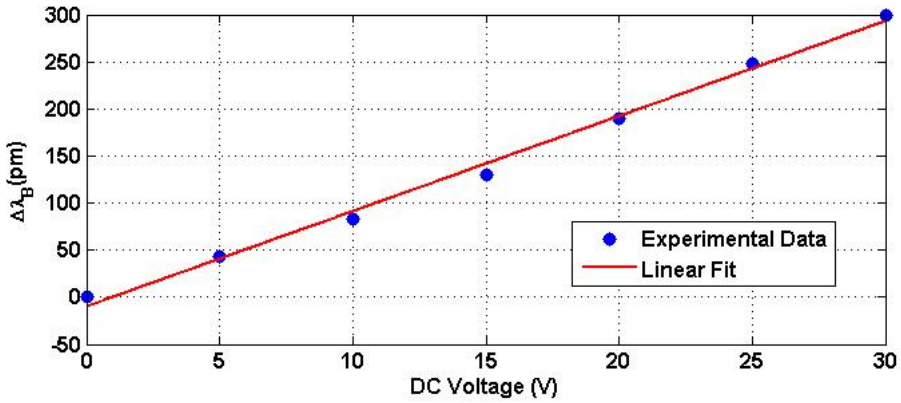

Figure 3.10: Shift in Bragg wavelength with increase in voltage

The slope obtained from the linear fit was 10 pm/V or 0.01 nm/V. The strain coefficient of the fibre is 1.3 pm/$\mu\epsilon$. So the strain per unit voltage 7.7 $\mu\epsilon$/V. So at different voltages we can evaluate the corresponding strain. From this strain we can calculate the corresponding path delay ΔL from which we can find out the applied phase change.

$$\frac{(\Delta L)}{L} = (7.7\mu\epsilon/V) \times (AppliedVoltage(V)) \tag{3.2}$$

In Eqn 3.2 L is the length of the FBG which is 3mm. Hence by calculating ΔL in nm we can find the corresponding applied phase change as shown in Eqn 3.3.

$$\Delta\phi = \frac{2\pi \times \Delta L}{1550} \tag{3.3}$$

We applied three different voltages in our experiment and using Eqn 3.2 and Eqn 3.3 measured the corresponding phase change applied mentioned in Table 3.1.

Applied DC voltage(V)	Delay(nm)	Applied Phase Change(mrads)
0.2	4.62	18.7
0.4	9.24	37.4
0.6	13.86	56.1

Table 3.1: Applied phase change for different DC voltages

The set-up for the experiment is shown in Fig 3.11

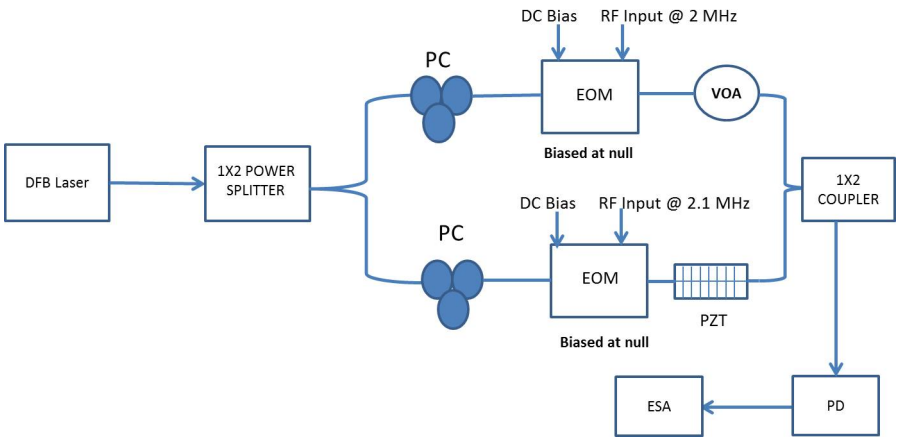

Figure 3.11: Experimental set-up for adding phase in one arm of self-synchronous LOCSET model

So as mentioned in Table 3.1 we applied the three mentioned voltages on the PZT. To estimate the phase change at the output we also observed the RF spectrum when no voltage was applied and it served as a reference. The comparison of the RF spectrum for the different applied voltages on the PZT with the unstrained case is illustrated in the plots below.

- Applied voltage on PZT 0.2 V

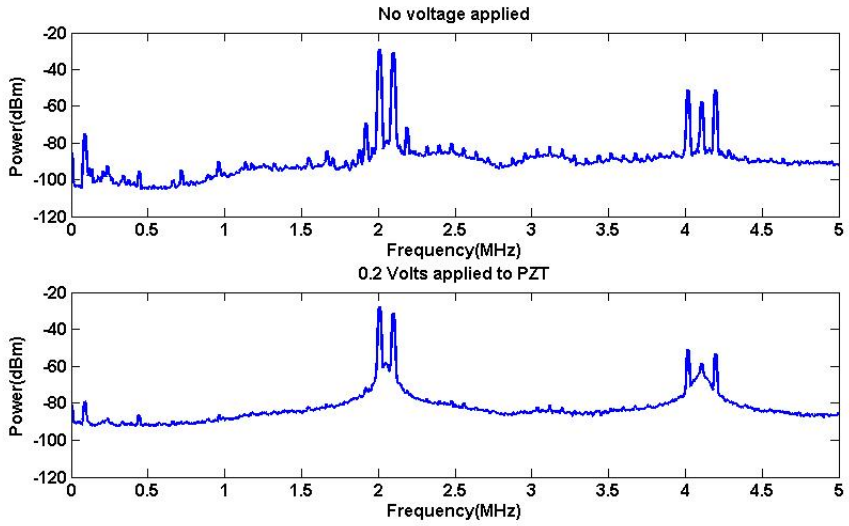

Figure 3.12: Comparison of peak levels for the unstrained case and when 0.2 V is applied on PZT

- Applied voltage on PZT 0.4 V

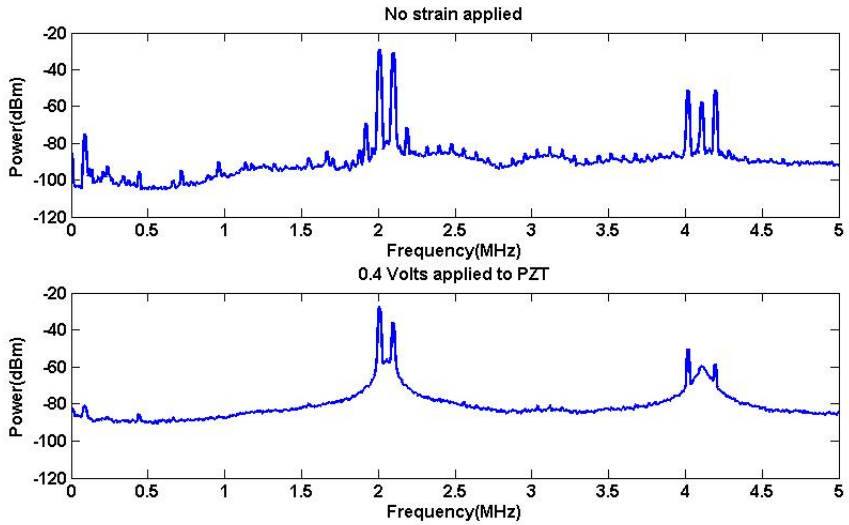

Figure 3.13: Comparison of peak levels for the unstrained case and when 0.4 V is applied on PZT

- Applied voltage on PZT 0.6 V

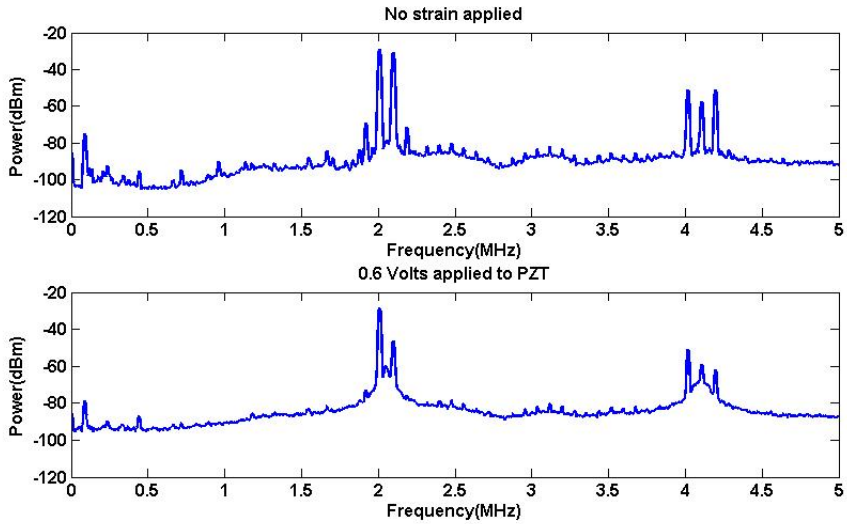

Figure 3.14: Comparison of peak levels for the unstrained case and when 0.6 V is applied on PZT

Hence we estimated the phase at the corresponding modulation frequencies for all these cases using Eqn 3.1. So we calculate the estimated phase change with respect to the reference case i.e. when no voltage is applied to the modulator and observe its dependence on the applied phase change. The plot shown in Fig. 3.15 shows the correlation between the applied and estimated phase change for three different voltage cases.

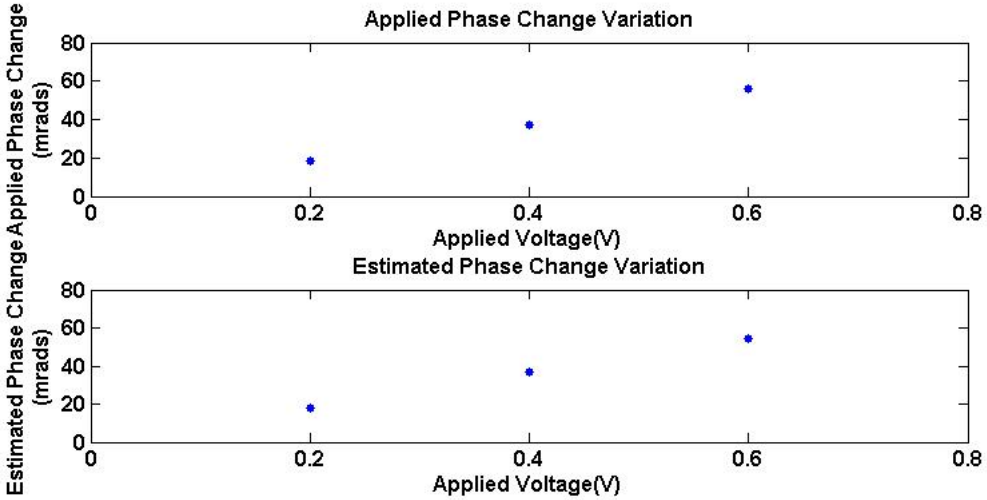

Figure 3.15: Comparison of applied and estimated phase changes for 3 different applied voltages

However the estimated phase changes due to the three different voltages will have minute fluctuations over a range of time as the peak levels will vary with time. Hence

to take this into account we estimated the phase for each voltage for 100 iterations and estimated the phase each time. Next we found out the corresponding estimated mean phase change. Eventually we obtained 3 arrays corresponding to the 3 voltages, each of them having 100 values of estimated phase change. Using this data we obtained the histogram of each of these arrays along with mean ($\mu_{\Delta\phi_{est}}$) and standard deviation ($\sigma_{\Delta\phi_{est}}$). Hence the results obtained from the above analyses can be tabulated as shown in Table 3.2 .

Applied DC voltage(V)	Applied Phase Change(mrads)	Mean estimated phase change $\mu_{\Delta\phi_{est}}$(mrads)	Standard Deviation of estimated phase change $\sigma_{\Delta\phi_{est}}$(mrads)
0.2	18.7	17.6	1.134
0.4	37.4	36.5	1.154
0.6	56.1	54.2	1.178

Table 3.2: Tabulation of estimated phase change

From the plots in Fig. 3.15 it is evident that the estimated phase change also varies linearly with the voltage similar to the applied phase change which is a linear function of the applied DC voltage. Infact the estimated phase change also satisfies a linear function with the applied voltage. At the same time these two phase changes are also linear with respect to each other which is shown in Fig. 3.16.

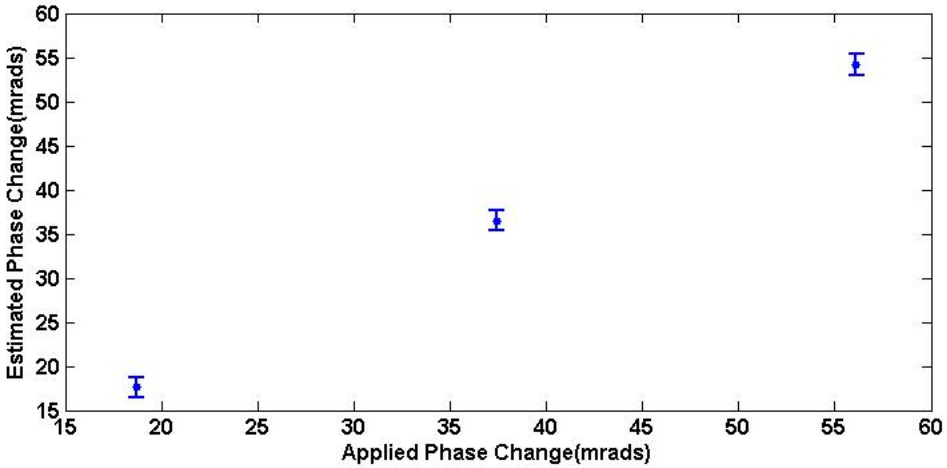

Figure 3.16: Variation of estimated phase change with the applied phase change

The above plot justifies the linear nature of the estimated phase change with respect to the applied phase change. The standard deviation of the estimated phase change are denoted by the error bars in Fig. 3.16.

Hence from this experiment we can conclude that the linearity of the estimated phase change with the applied phase change is established and which is depicted in Fig. 3.16. From this experiment we can conclude that if a phase change is applied in one of the arms, which is a fraction of π we can observe a parallel change in the estimated phase at the output. At the same time to get an idea of the subsequent errors that incur while measuring the estimated phase change, the standard deviation calculation plays a vital role.

CHAPTER 4

Conclusion and Future work

In this project we have been able to successfully establish the MATLAB-SIMULINK model for 2-beam self-referenced LOCSET schematic. The model has helped us to understand the photo-current response with time. Using the SIMULINK model we also developed a phase estimation schematic, to estimate the phase at the output after providing a certain input phase. The phase estimation methodology helped us to have an idea of the phase error incurred and its variation with different input phase values. The phase error dependence on the input phase also helped us to quantify the limit of the maximum permissible phase error.

Being able to estimate the phase from simulations, our next aim was to carry out some controlled experiments on both self-synchronous and self-referenced schematics and estimate the phase at the output correspondingly. In this regard we utilised two EOMs as our phase modulators by biasing them at their null position. So we successfully observed the RF spectrum for both the 2-beam self-referenced and 2-beam self-synchronous LOCSET on the ESA. Incorporating the same analogy as used in simulations we estimated the phase at the output of both the arms of the self-synchronous model which were modulated at two unique RFs 2 and 2.1 MHz. Hence we could estimate the phase at the output and at the same time evaluate the phase error with respect to the applied input phase. To further extend our analysis, we introduced additional phase in one of the arms using a PZT and correspondingly evaluated the change in the estimated phase. It was seen that with the increase in delay, the peak levels for the fundamental and second harmonics of the modulation frequency got reduced and from that change we were able to estimate the phase change.

Our primary aim is to obtain high power at the output by phase-locking all the individual optical array elements. So our future work will focus on finding a suitable DSP locking mechanism which would able to lock back the individual phase errors back into the phase modulators. Apart from that in order to achieve higher optical powers we need to incorporate Erbium Doped Fiber Amplifiers (EDFAs) in each of the arms. But

the EDFAs owing to ASE will lead to additional phase noise. Hence it is prerogative to design a robust DSP phase locking module which would be able lock back the phase noise into the individual phase modulators. The basic phase locking model is discussed below.

Normally in coherent beam combining using self-referenced LOCSET technique we use a large number of fiber amplifiers and finally phase locking is implemented. The model shown in Fig 4.1 looks into a 2 element array in which one of the beams is un-modulated and the other is modulated by using a phase modulator.

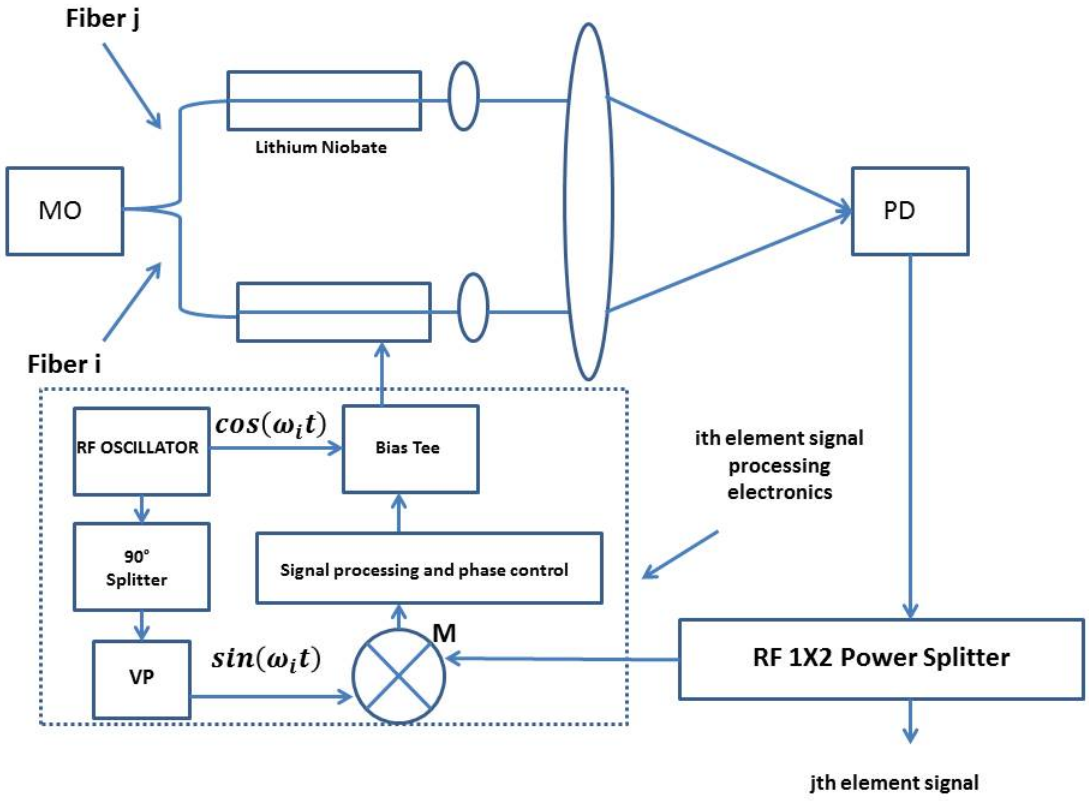

Figure 4.1: Block diagram for the phase-locking electronics of a 2-element array

In the setup shown above both the array elements have their own RF phase modulation frequency. The photocurrent obtained from the photo-detector is incident on the 1x2 RF power splitter and then the output signals from it are then transferred to two independent signal processing circuits one for fiber i and the other for j(not shown here). Only difference between these two signal processing circuits is that for fibers i and j are the phase modulation frequencies ω_i and ω_j. The signal processing unit carries out two functions:-

- Small RF phase modulation is applied to the phase modulator for a single array element.
- The optical phase error signals are extracted for that particular element and fed back to the phase modulator to cancel phase variations in that array element.

In this self-referenced mode the phases of the phase modulated array elements are adjusted by the feedback loop to track the phase of the un-modulated element. Therefore the relative phases between the un-modulated array element and each of the phase modulated array elements at the sensing photo-detector are preserved when any or all of the array elements are disturbed. In the setup shown above the RF coherent demodulation is manifested by using a mixer M to multiply the photo-detector current times $\sin(\omega_i t)$ and then integrating the output of the mixer over many cycles of the RF frequency for that array element. Eventually the model is able to phase lock each element of the array to the same phase of the other array elements [(4)].

APPENDIX A

SIMULINK model and other MATLAB simulations

A.1 2-beam Self-referenced LOCSET model

Fig.2.1 is the illustration of the original SIMULINK model shown below:-

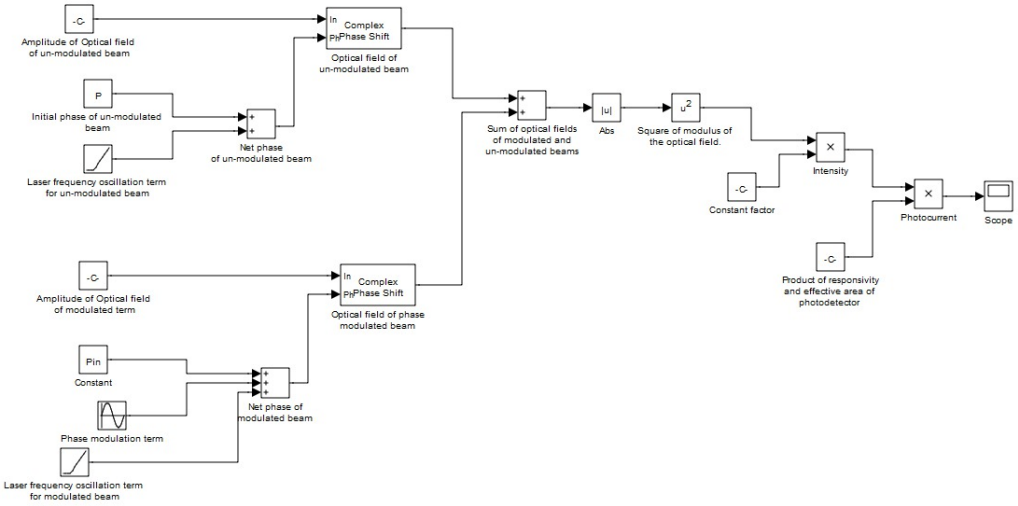

Figure A.1: SIMULINK model for 2-beam self-referenced LOCSET

The model shown in Fig.A.1 shows the addition of two optical fields- one un-modulated and the other phase modulated being tagged to a certain RF. In this model we can see there are 2 blocks called **Complex Phase Shift** which adds phase to a constant term. Hence we can see it has two input ports - one for the amplitude and the other for the phase. For the un-modulated case we have two input phase terms - one the initial phase of the un-modulated beam and the other corresponding to the laser frequency, $\omega_L t$. For the phase modulated case there are three input phase terms, the extra being the modulation term, $\beta \sin(\omega_{RF} t)$. Finally the optical fields of both these beams are added followed by modulus square. The result obtained from this operation is multiplied by the constant factor $\frac{1}{2}(\frac{\epsilon_0}{\mu_0})^{\frac{1}{2}}$ which gives us the intensity. Upon multiplying the intensity with the product of responsivity, R_{PD} and effective area, A of the photodetector we eventually obtain the photocurrent and its time response is observed in the **Scope**.

A.2 MATLAB code for 2-beam self-synchronous LOC-SET model

```
clc
clear all
% close all

figure;
dt=4e-9;
t=dt:dt:1e-3;
v_p1=3.2;  % V_pi of first EOM
v_p2=3.1;  % V_pi of second EOM
extn1=2512;  % Extension Ratio of first EOM
extn2=1995   % Extension Ratio of second EOM

v_p_p1=0.09; % Amplitude of the RF signal
v_p_p2=v_p_p1;

f_p_1=2e6;  % Modulation frequency of first EOM
f_p_2=2.1e6 % Modulation frequency of second EOM


R_pd=0.85;  % Responsivity of Photodetector
propconst=2.654e-3; % 0.5*sqrt(epsilon_0/mu_0)
effarr=20e-12;       % Effective area of Photo Detector

del1=(sqrt(extn1)-1)/(sqrt(extn1)+1);
del2=(sqrt(extn2)-1)/(sqrt(extn2)+1);

v1=v_p_p1*sin(2*pi*f_p_1*t)-5.6;
v2=v_p_p2*sin(2*pi*f_p_2*t)-4;

```

```
30 e1=(sqrt(10^(-4.595)/2)).*(exp((j*pi*v1/(2*v_p1)))+del1*
       exp((-j*pi*v1/(2*v_p1))));  %Optical field of one arm
31 e2=(sqrt(10^(-4.595)/2)).*(exp(j*pi*v2/(2*v_p2))+del1*exp
       (-j*pi*v2/(2*v_p2)));  %Optical field of second arm
32
33 e_heterodyne=(e1+e2);
34 p_heterodyne=(abs(e_heterodyne)).^2;
35
36
37
38 fs=1/dt;
39 f=linspace(-fs/2,fs/2,length(t));
40 fft_p_heterodyne=abs(fftshift(fft(p_heterodyne.*(R_pd*
       effarr*propconst))));%Computing FFT
41
42
43
44 figure;
45 plot(t*1e6,p_heterodyne);
46 figure;
47 plot(f/1e6,log10(fft_p_heterodyne)); % Plotting the RF
       spectrum
48 xlim([-5  5]);
49 ylim([-30  -8]);
```

The above code implements the 2-beam self-synchronous LOCSET model which helped us to understand the theory behind this technique. Analogous to the experiments we will obtain peaks at the first and second harmonics of the modulation frequencies. The RF spectrum obtained from the simulation is shown in Fig. A.2.

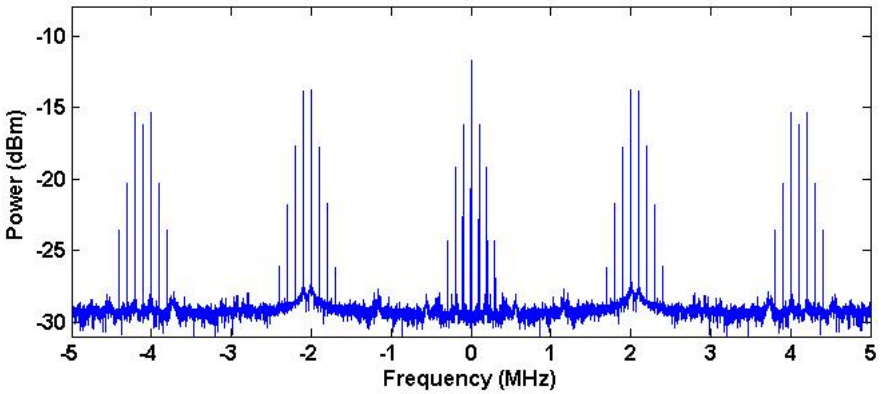

Figure A.2: RF spectrum for 2-beam self-synchronous model obtained from MATLAB code

REFERENCES

[1] Hagop Injeyan, Gregory D. Goodno, *High Power Laser Handbook*, McGraw Hill,2011.

[2] C.D. Nabors, *Effects of phase errors on coherent emitter arrays*, Applied Optics, 33(12), April 1994

[3] Tso Yee Fan, *The Effect of Amplitude (Power) Variations on Beam Combining Efficiency for Phased Arrays*, IEEE Journal of selected topics in quantum electronics, 15(2), March/April 2009

[4] Thomas M. Shay, Senior Member, IEEE, Vincent Benham, Jeffrey T. Baker, Anthony D. Sanchez, D. Pilkington, and Chunte A. Lu, *Self-Synchronous and Self-Referenced Coherent Beam Combination for Large Optical Arrays*, IEEE Journal of selected topics in quantum electronics, 13(3), May/June 2007

[5] Thomas M. Shay, *Theory of electronically phased coherent beam combination without a reference beam*, Optics Express, 14(25), December 2006